6. DISCUSSION OF RESULTS

6.1 Discussion of Results for Ru/SiO_2 Catalysts

6.1.1 Preliminary Experimentation

During the room-temperature CO-deposition process onto the Ru/SiO_2 catalyst, formation of CO_2 was not detected. If, under the conditions of the adsorption process (1 atm, 298 K), atomic carbon is deposited via the Boudouard reaction, then one would expect to detect CO_2 formation upon exposure to CO. Conversely, if the CO adsorbs molecularly on the catalyst surface, then no CO_2 would be expected to form. In addition, the formation of water upon exposure of the catalyst to hydrogen requires the presence of adsorbed oxygen. For these reasons, it is assumed that the CO adsorbed on the catalyst in this study does so without loss of the oxygen. Early studies by Rabo [108] also did not detect CO disproportionation to CO_2 during room temperature adsorption of CO over silica-supported Ru. This study also noted that no reaction took place upon exposure of this chemisorbed CO to hydrogen gas at room temperature. As mentioned previously, such low temperature adsorption on ruthenium is believed to be molecular and not dissociative, resulting in a metal-to-CO ratio of 1:1. It is possible that dissociation of the molecularly adsorbed CO may occur upon heating of the catalyst surface to reaction temperatures prior to exposure to hydrogen. However, since this dissociation would require formation of metal-oxygen bonds on a surface already saturated with chemisorbed CO, dissociation would require desorption of CO as metal-carbon bonds are broken in favor of metal-oxygen bonds. As desorption of

CO during heating was not observed, it is assumed that the metal to carbon ratio remained at unity. Duncan [109] and Mizushima [110] both reported that CO desorption from supported Ru catalysts does not occur until about 573 K, while Yamada and Tamaru [41] report CO desorption from Ru single crystal surfaces at 480 K.

Deactivation of the Ru surface through irreversible atomic carbon deposition was not found to occur to a detectable degree under the conditions of these experiments, as evident from the relatively constant calibration factor values obtained for each experiment. The calibration factors are equal to the integrated area under the total methane (mass spectrometer) signal for each experiment as the reaction is driven to completion, and this area is directly proportional to the total amount of methane formed. Had appreciable deactivation been occurring through the course of the experiments, less and less methane would be formed with each successive experiment, and one would expect to see a change in the calibration factors to lower values.

6.1.2 Methanation Reactions

The turnover frequencies obtained in this study are similar to those obtained by others in steady-state experiments, as shown in Table 4 [15, 24, 111-113], where the maximum TOF for this study is listed for comparison with the higher temperatures of other studies. The deviation from linearity in the TOF at high temperatures is likely due to diffusion effects interfering with the spectrometer response at these temperatures, limiting the maximum measurable TOF in this system to around 0.01 s^{-1}. Fortunately, these are the highest rates monitored during the course of this research, since the addition of other metals to Ru results in significantly lower TOF values.

6.1.3 Kinetic Parameters

The value of the activation energy, 23.2 kcal/mole, is also in good agreement with the steady-state results of others. Since the rate-determining step in the mechanism of CO hydrogenation is the hydrogenation of surface carbon species, the adsorption of CO does not affect kinetic results. Therefore, comparison of results from steady-state studies and experiments which utilize preadsorbed CO is justified.

6.1.4 ^{1}H-NMR Experimentation

Previous studies by our group have identified three hydrogen-on-ruthenium resonances in ^{1}H-NMR adsorption studies [44]. They have been labeled and described as: α_I, strongly bound, low pressure hydrogen (-60 ppm); α_M, weakly bound, low pressure hydrogen; and β, weakly bound, high pressure hydrogen. The α_I, α_M and β resonance peaks occur at shifts of about -60 ppm, -55 ppm and -45 ppm, respectively. The two resonance peaks found in Figure 7 appear to correspond to the weakly bound α_M and β hydrogen

TABLE 4. Comparison of kinetic parameters for methanation over supported Ru

author	**support**	**temp (K)**	**pressure (atm)**	**E_a (kcal/mol)**	**CH_4 TOF (mol /site /s)**
Della Betta [111]	Al_2O_3	473 -610	0.76	24	0.020 (548 K)
Vannice [15]	Al_2O_3	478-503	1.0	24.2 ± 1.2	0.181 (548 K)
Vannice [113]	SiO_2	478-503	1.0	27.0	0.068 (548 K)
Ekerdt [112]	SiO_2	465-550	-	24.1	0.130 (548 K)
Goodwin [24]	SiO_2	510-540	0.76	19.5	0.013 (510 K)
this study	SiO_2	400-500	0.61	23.2 ± 1.8	0.010 (500 K)

species. These two hydrogen species are known to exchange rapidly with the gas phase, and the β species is thought to be an absorptive precursor to the α species, and is thus partially associated with gas phase hydrogen [44].

The asymptotic hydrogen coverage of 2.5 H/Ru_s in Figure 9 has been confirmed by previous studies on this catalyst [43] in the absence of adsorbed CO, and by unpublished work by our group during reaction with preadsorbed CO. Direct comparison of this data with that from CO-free adsorption studies is justified since it has been shown that the surface carbon is nearly completely depleted after 30 minutes. For this reason, the higher coverage data in this figure represents hydrogen adsorption on a surface with very little CO present.

If experimental conditions are such that few unoccupied sites exist on the catalyst at any given time, and that any products formed rapidly desorb, then $\theta_{CO} \approx 1 - \theta_H$ and equation 3 simplifies to:

$$rate = k\left(\theta_H - \theta_H^2\right) \tag{13}$$

This equation is consistent with the data in Figure 9, which shows a symmetric increase and decrease in the rate about a central coverage of hydrogen. The first and second derivatives of equation (13) show that the maximum rate should occur at $\theta_H = 0.5$. However, since θ represents relative coverages, it's value is limited between 0 and 1, while H/Ru_s is not limited, and varies from 0 to 2.5 under these conditions. If it is assumed that an H/Ru_s coverage of 2.5 corresponds approximately to $\theta_H = 1$, then the rate should maximize at $H/Ru_s = 1.25$, which is not far from the observed value of 1.1. Therefore, it appears that the kinetic derivations presented earlier are supported by these NMR results.

6.2 Discussion of Results for Ag-Ru/SiO_2 Catalysts

6.2.1 Methanation Reactions

The background information previously presented on bimetallic Group IB-Ru catalysts stressed the dramatic effect addition of the Group IB metal has on the catalytic behavior of transition metals, and this effect is well represented in Figure 10. Previous CO hydrogenation studies on silica-supported Group IB-Ru catalysts by our group [88] also reported large decreases in activity for the Ag-Ru series, with the TOF for CO consumption decreasing rapidly up to a Ag content of 20 %. At higher Ag loadings, only marginal decreases were evident. Our Monte-Carlo simulations of Ag-Ru catalysts indicate that this loading corresponds to nearly complete occupation of all low-coordination sites by Ag.

Table 5 compares these results with those of previous similar studies. Although this table shows wide variations in the measured effect of Ag addition on reaction rates, the general trend of a strong reduction in the specific activity of Ru is same in all cases, even at Ag loadings as low as 10%. To the author's knowledge, no activation energy measurements for CO hydrogenation have previously been made on Ag-Ru catalysts for comparison.

TABLE 5. Rate decreases during CO hydrogenation upon addition of Ag to Ru catalysts

author	support	temperature	pressure	Ag content	TOF change
Enomoto [76]	Al_2O_3	493 K	0.66 atm	50 %	-76 %[a]
Kelzenberg [88]	SiO_2	523 K	11.0 atm	13 %	-18 %[a]
				30 %	-58 %[a]
this study	SiO_2	473 K	0.61 atm	10 %	-76 %[b]
				30 %	-93 %[b]

[a] for CO consumption
[b] for CH_4 formation

6.2.2 Kinetic Parameters

The observed decrease in apparent activation energy for CO hydrogenation upon addition of Ag to Ru/SiO$_2$ in Figure 12 can be interpreted as follows. The reaction rate for methane production in this system is given by equation (6):

$$rate = \frac{k\left(K_H P_H\right)^{1/2} K_{CO} P_{CO}}{\left[1 + \left(K_H P_H\right)^{1/2} + K_{CO} P_{CO}\right]^2} \tag{6}$$

Since CO adsorption is very strong, K_{CO} is quite large, and $K_{CO}P_{CO} \gg 1 + (K_H P_H)^{1/2}$, so:

$$rate \approx \frac{k\left(K_H P_H\right)^{1/2}}{K_{CO} P_{CO}} \tag{14}$$

The form of this equation is quite similar to those of other researchers presented earlier in equations (1) and (2), where the reaction orders are frequently positive with respect to hydrogen and negative with respect to carbon monoxide.

The equilibrium constants for adsorption are given by:

$$\ln K^{1/2} = -\frac{\Delta G_{ads}}{2RT} \tag{15}$$

Combination of equation (12) and substitution (14) into equation (13) yields:

$$rate = \left[\frac{ek'T}{h}\frac{P_H^{1/2}}{P_{CO}}\exp\left(\frac{\Delta S^\circ}{R}\right)\right]\exp\left(-\frac{\left(E_a + \frac{1}{2}\Delta G_{ads}^{H_2} - \Delta G_{ads}^{CO}\right)}{RT}\right) \tag{16}$$

Substitution of the thermodynamic relation $\Delta G = \Delta H - T\Delta S$ gives the final result:

$$rate = \left[\frac{ek'T}{h} \frac{P_H^{1/2}}{P_{CO}} \exp\left(\frac{\left(\Delta S^\circ + \frac{1}{2}\Delta S_{ads}^{H_2} + \Delta S_{ads}^{CO} \right)}{R} \right) \right] \exp\left(- \frac{\left(E_a + \frac{1}{2}\Delta H_{ads}^{H_2} - \Delta H_{ads}^{CO} \right)}{RT} \right) \quad (17)$$

This equation shows that the observed activation energy, $E_{a,obs}$, obtained experimentally from an Arrhenius relation of the form:

$$\ln rate = -\frac{E_{a,obs}}{RT} + \ln c \quad (18)$$

is related to the heat of hydrogen adsorption by [27]:

$$E_{a,obs} = E_a + \frac{1}{2}\Delta H_{ads}^{H_2} - \Delta H_{ads}^{CO} \quad (19)$$

In effect, equation (19) shows that in a system where the kinetics of a rapid surface reaction are being slowed due to decreased reactant adsorption rates (manifested in an increase in the adsorption enthalpy of the reactants), the observed activation energy will be less than in the previous case (since adsorption is exothermic) [26-27]. While necessary for accuracy, the enthalpy term for CO adsorption in this expression is constant in this study since it is preadsorbed prior to reaction. Figure 13, adapted from Moulijn [27], is a graphical representation of this equation, where the CO adsorption enthalpy does not enter into the description.

Since the variables in these equations are all dependent upon hydrogen coverage, it is important to note that variables such as ΔH_{ads} are more accurately written as dH_{ads}, since they represent differential values over a given range of coverages. However, for simplicity, the integral representation for the variables will continue to be used. Comparison of equations (17) and (18) to yield equation (19) requires that the entropy terms are either

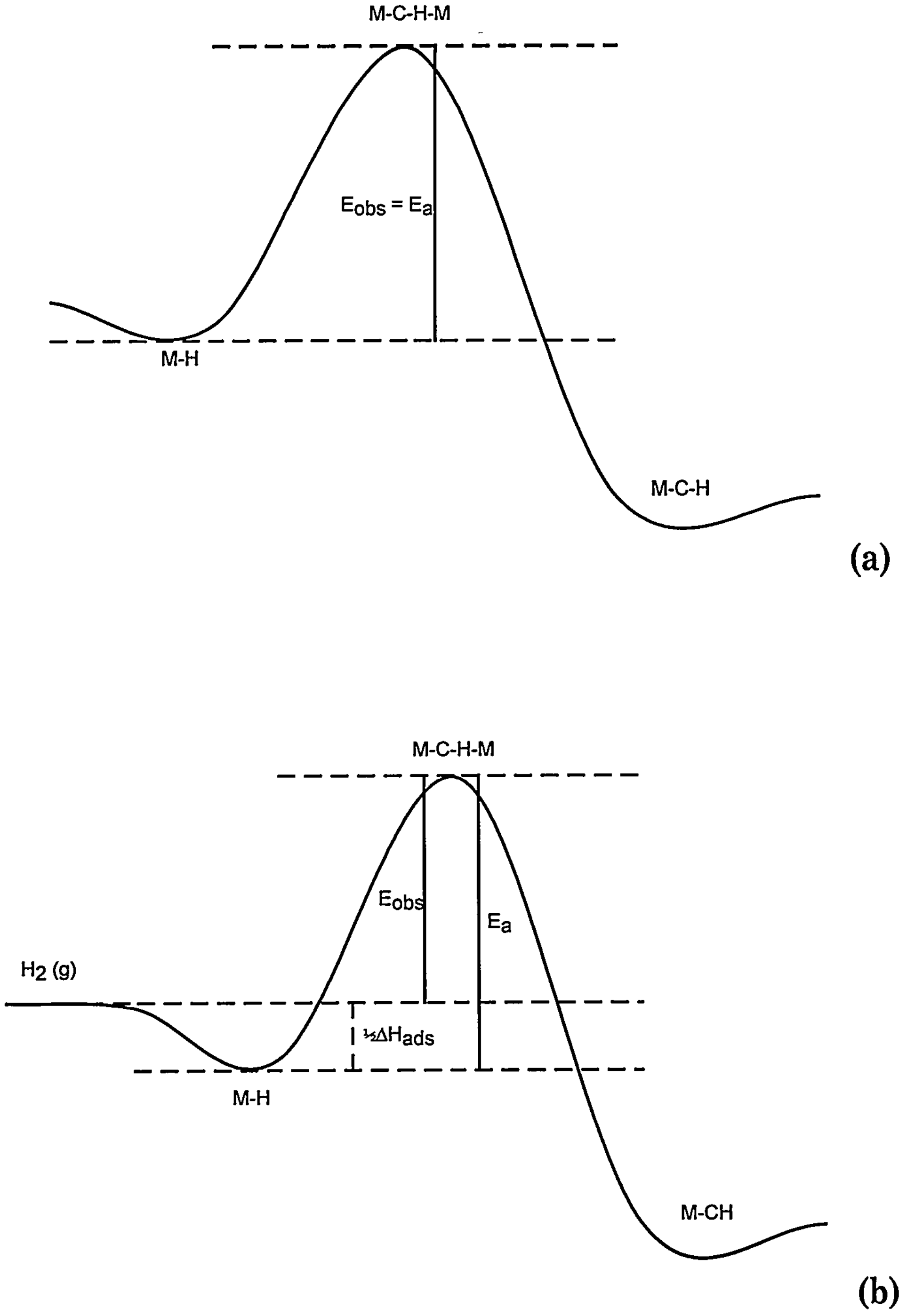

FIGURE 13. Differences in observed activation energy for a surface reaction (a) without adsorption influences and (b) with adsorption influences.

approximately constant within the temperature range considered, or at least that these terms are small enough in magnitude compared to the activation energy and enthalpy to be considered constant. The exponential temperature dependence of the enthalpy term will obviously be larger than the entropy term, which does not contain a temperature factor, apart from its own temperature dependence. The second requirement is generally true for such systems, and for hydrogen adsorption on the catalysts in this study, ΔH_{ads} ranges between -5 and -95 kJ/mol, while ΔS_{ads} ranges from -20 to -170 J/mol K [99].

Microcalorimetry data gathered by our group on these catalysts, reproduced in Figure 14 [99], shows that the differential heat of adsorption for hydrogen on the Ru and Ag-Ru catalysts at 400 K decreases with increasing hydrogen coverage and Ag content. The ^{1}H-NMR results for the monometallic catalyst presented earlier indicate that the steady-state coverage at 400 K is between 1.0 and 1.1 H/Ru$_s$. This also corresponds to a differential heat of adsorption of approximately -50 kJ/mol. Except for very low (initial) coverages, the adsorption enthalpy is higher at all coverages on the bimetallic catalysts. Since the presence of silver acts to increase the heat of adsorption of hydrogen, this figure shows that adsorption enthalpies greater than -50 kJ/mol (the monometallic case) correspond to hydrogen coverages between 0.25 and 0.60 H/Ru$_s$ before the enthalpy becomes negligible.

Clearly, the amount of hydrogen available on the surface for reaction is strongly reduced in the presence of silver, from about 1.1 H/Ru$_s$ for Ru/SiO$_2$ to between 0.25 and 0.60 H/Ru$_s$ in the Ag-Ru series. This corresponds to an increase in the differential heat of adsorption for hydrogen from about -50 kJ/mol in the monometallic case to between -10 and

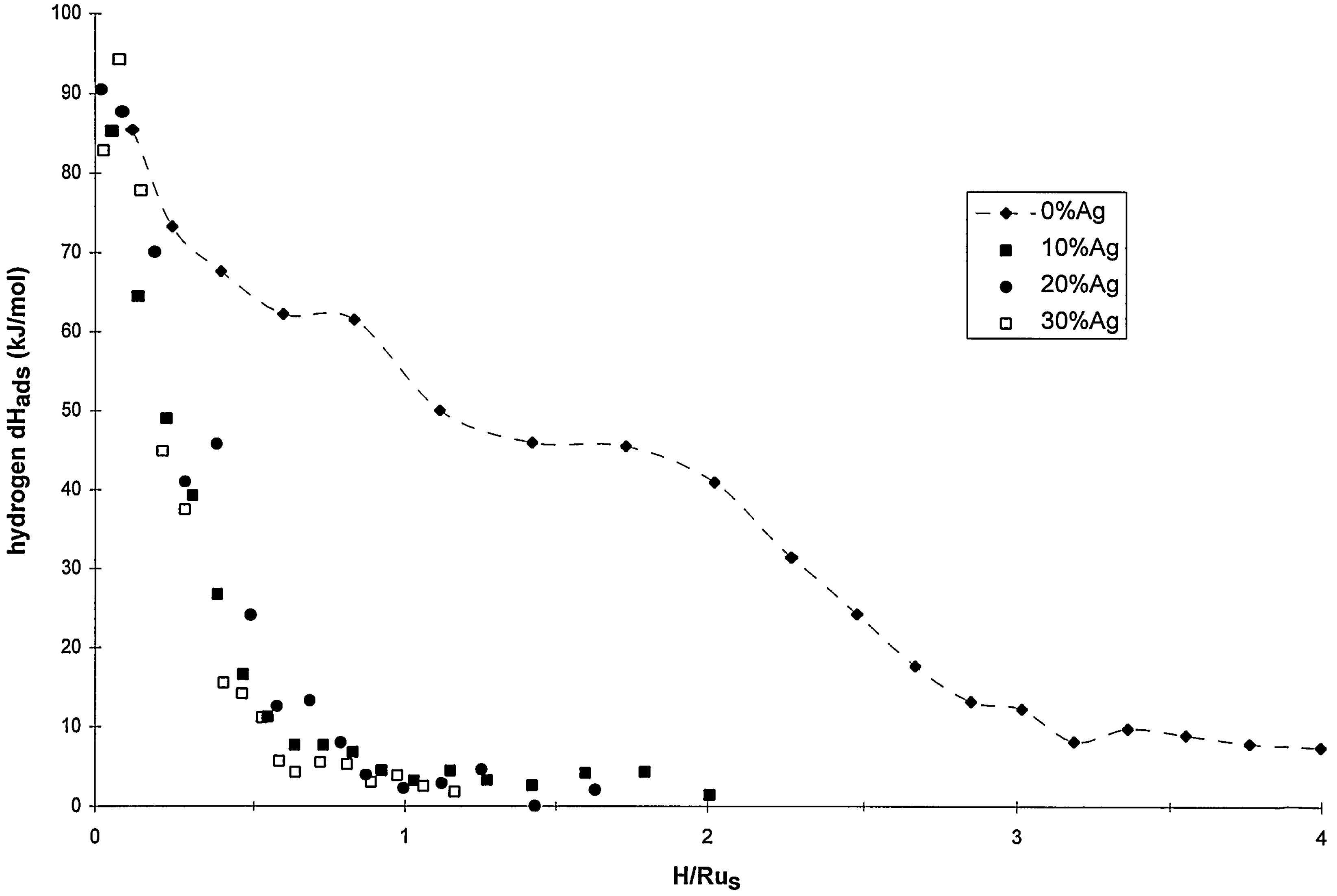

FIGURE 14. Differential hydrogen adsorption enthalpy on Ag-Ru/SiO_2, 403K (Narayan and King, 1998)

-40 kJ/mol in the bimetallic series. This behavior is reflected in changes in the integral adsorption enthalpies for these catalysts. The microcalorimetric studies by our group [99] revealed a net increase in the integral heat of hydrogen adsorption upon addition of Ag to Ru/SiO_2.

These results may shed further light on reported differences in the kinetics of CO hydrogenation between Ag-Ru and Cu-Ru systems. While previous measurements of activation energies during CO hydrogenation have not been conducted on Ag-Ru catalysts, the results of this study clearly indicate an apparent decrease in the observed activation energy at all levels of Ag loading. However, previous studies of Cu-Ru systems have reported either no change in activation energy [78, 90] or slight increases [88, 89]. In both systems, large decreases in specific Ru activity have been reported. The apparent disparity in measured activation energies between these two systems may be accounted for by differences in hydrogen adsorption characteristics of these systems. While neither Ag or Cu adsorbs hydrogen appreciably, spillover of hydrogen from Ru is known to occur for Cu [79], but not for Ag [51]. While the exact effects of this difference have not yet been completely elucidated, the ^{1}H-NMR study of Wu [51] showed that Cu interacts with Ru more strongly that Ag, with less Cu than Ag being required to cover the same fraction of surface Ru. Chen [80] description of Cu as acting as a "holding area" for hydrogen spillover to accommodate CO hydrogenation to CH_x species supports the observation of increased CH_4 selectivity by Cu during CO hydrogenation [78, 89, 90].

7. PORTAL SITE MEDIATED HYDROGEN ADSORPTION

The observed decrease in the specific activity of Ru in Ag-Ru systems in this study may be explained in terms of a phenomenon termed "portal site mediated adsorption" by our group [99, 114]. Figure 15 is a schematic of the operative surface processes in this model. According to the model, hydrogen adsorption occurs via two pathways. The first involves rapid, dissociative adsorption at low-coordination sites to produce weakly-bound, highly mobile hydrogen. Similar adsorption and dissociation behavior has been shown to be more

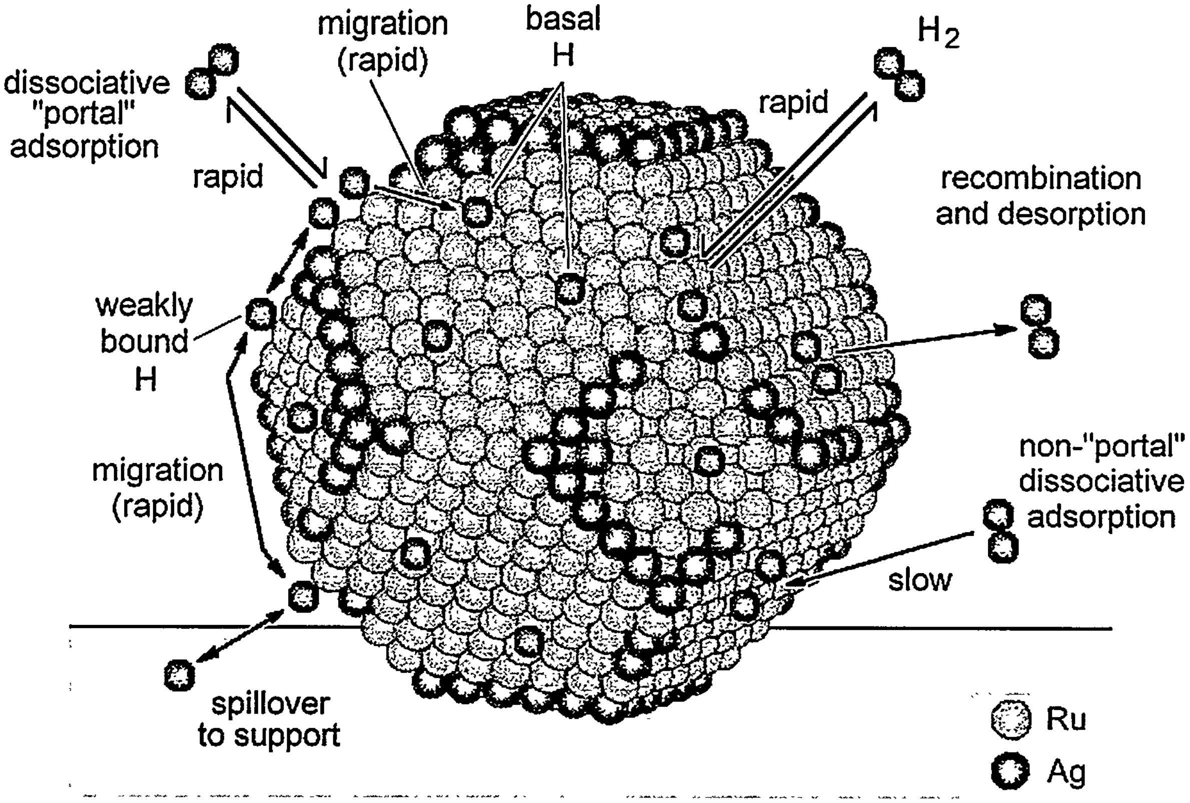

Figure 15. Portal site mediated adsorption of hydrogen

efficient at low-coordination sites on platinum [70]. The second pathway is adsorption directly onto the basal planes, which occurs at an intrinsically slower rate [76]. Since the weakly-bound hydrogen adsorbed at low-coordination sites is highly mobile, it can then either: (1) migrate to strongly-bound states, (2) spillover to the support, or (3) recombine with another hydrogen atom and desorb.

In the presence of adsorbed CO, the portal sites serve as "sinks" for gaseous hydrogen, supplying weakly-bound, mobile surface hydrogen for reaction. When Ag occupies portal sites, it effectively closes the portals to hydrogen adsorption. Hydrogen must then adsorb directly onto the basal planes, a process which, as mentioned, occurs more slowly. Recombination and desorption of hydrogen, which is not affected to a large extent by the occupation of low coordination sites by Ag, continues simultaneously. The net effect is a slowing of methane production due to decreased availability of surface hydrogen, in effect altering the limiting kinetics of the overall process from surface reaction to adsorption of hydrogen.

Recent microcalorimetric studies on the adsorption of hydrogen onto silica-supported Ru and Ag-Ru catalysts by our group [99] support this model. In these studies, Narayan noted the following effects on addition of Ag to Ru catalysts:

1. no significant change in the initial heat of hydrogen adsorption, 90 to 95 kJ/mol (Figure 14);
2. the total amount of hydrogen adsorbed per ruthenium surface atom was significantly reduced (Figure 14);

3. the reduction in adsorbed hydrogen was coupled with a loss in weak and intermediate hydrogen adsorption states, between 40 and 60 kJ/mol (Figure 16); and
4. no significant change in the amount of strongly-adsorbed hydrogen states above 80 kJ/mol (Figure 16).

The fact that the initial heat of adsorption for these both types of catalysts are essentially the same suggests the absence of electronic ("ligand"), ensemble or segregation effects which directly affect the chemisorptive bond or adsorption site. Other studies by our group using ^{1}H-NMR support the lack of electronic [46] or ensemble [88, 96, 100, 103] effects in Ag-Ru systems. This suggests that either low coordination sites do not have significantly different heats of adsorption, or that there are too few of these sites to resolve them in microcalorimetry [99].

Since it is known that Ag atoms preferentially occupy low-coordination edge and corner sites in Ag-Ru/SiO_2 catalysts, the observed loss of low to intermediate adsorption states is coupled with the loss of low-coordination sites for hydrogen adsorption on these surfaces. Several possibilities exist to explain this observation:

1. electronic effects;
2. blocking or other geometric site alterations; or
3. changes in the kinetics of hydrogen adsorption.

As previously discussed, electronic effects are not considered to be operative in this system. Although Ag blocks low coordination sites, these sites would each have to accommodate 10 to 20 hydrogen atoms to account for the large losses of hydrogen observed [99]. In addition, this second possibility is unlikely due to the previously mentioned high mobility of hydrogen

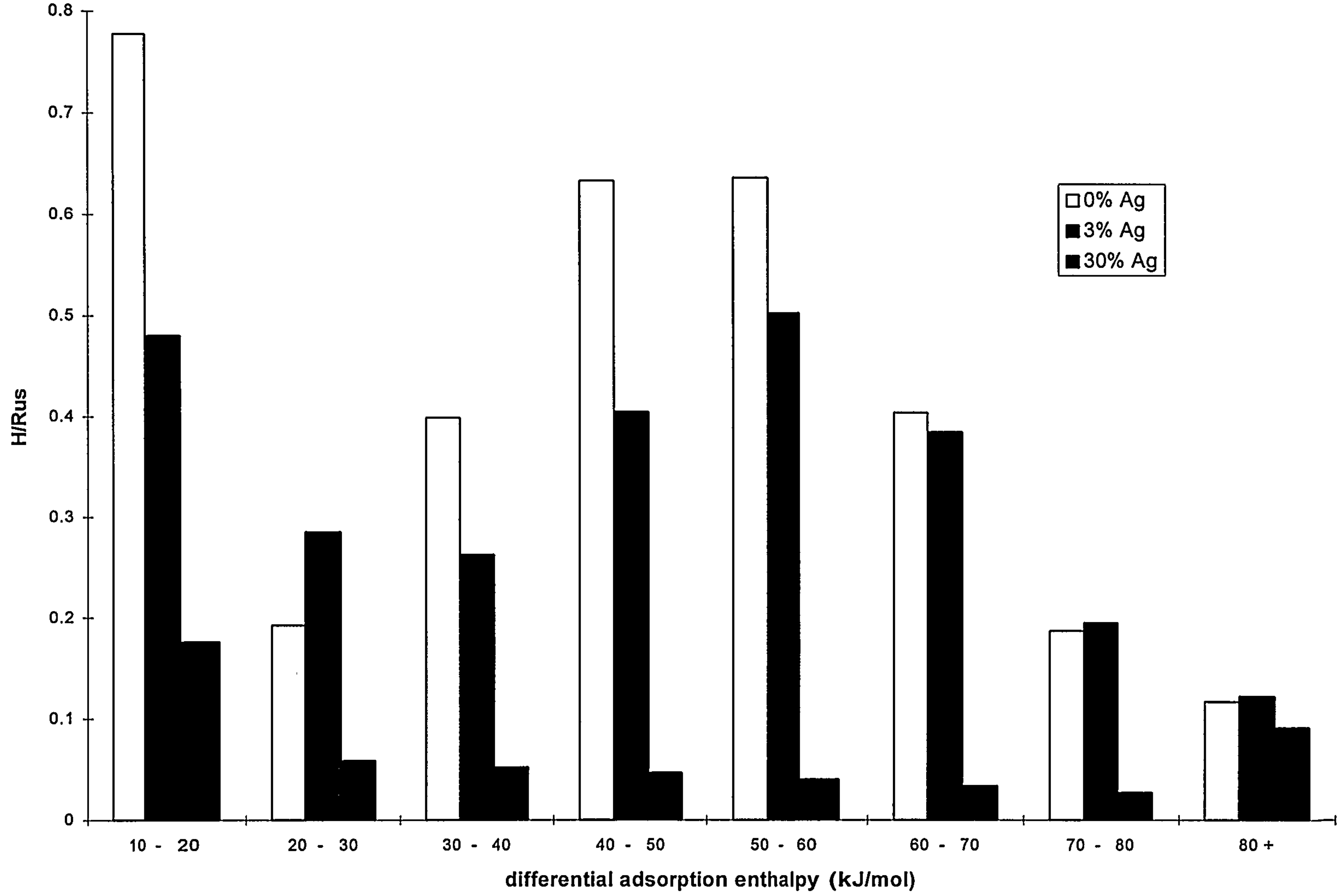

FIGURE 16. Differential adsorption enthalpy distribution (Narayan and King, 1998)

under these conditions. The third alternative is accounted for by the portal site mediated adsorption model. Under this model, any weakly-bound hydrogen that is able to adsorb either migrates to strongly-bound states, spills over to the support, or recombines and desorbs. The simultaneous recombination and desorption of surface hydrogen takes place at relative rates, according to the adsorption states of the two atoms combining:

weak-weak > weak-strong > strong-strong

Thus, the strongly-bound hydrogen remains on the surface longer and accumulates. However, since the replentification of weakly-bound surface hydrogen at portal sites is being blocked by Ag in the bimetallic system, the net effect is a depopulation of weakly-bound states, as evident in Figure 16.

This view is supported by results of recent studies using ^{1}H-NMR, which showed the rates of hydrogen adsorption being dramatically lowered on bimetallic catalysts [115] and decreases in measured hydrogen sticking coefficients on Ag-Ru [93]. In addition, the fact that the microcalorimetry results clearly show an increase in the average heat of adsorption of hydrogen on these catalysts supports the observations of previous reaction studies by our group. These studies [96, 103] showed a decrease in the order of reaction of hydrogen from -1.5 to -2.5 upon addition of Ag to Ag-Ru/SiO_2 during ethane hydrogenolysis, an effect which is the same as if the heat of adsorption of hydrogen was greater on the bimetallic catalyst [99]. See Kumar [116] for a more lengthy discussion of the application of the portal site adsorption model to ethane hydrogenolysis.